Neural fields models

John Wyller

Faculty of Science and Technology
Norwegian University of Life Sciences,
Ås, NORWAY

24.05.2017

Overview

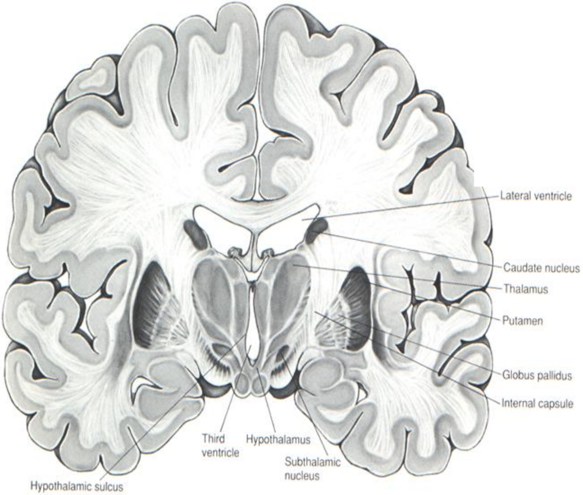
Lateral ventricle
Caudate nucleus
Thalamus
Putamen
Globus pallidus
Internal capsule
Third ventricle
Hypothalamus
Subthalamic nucleus
Hypothalamic sulcus

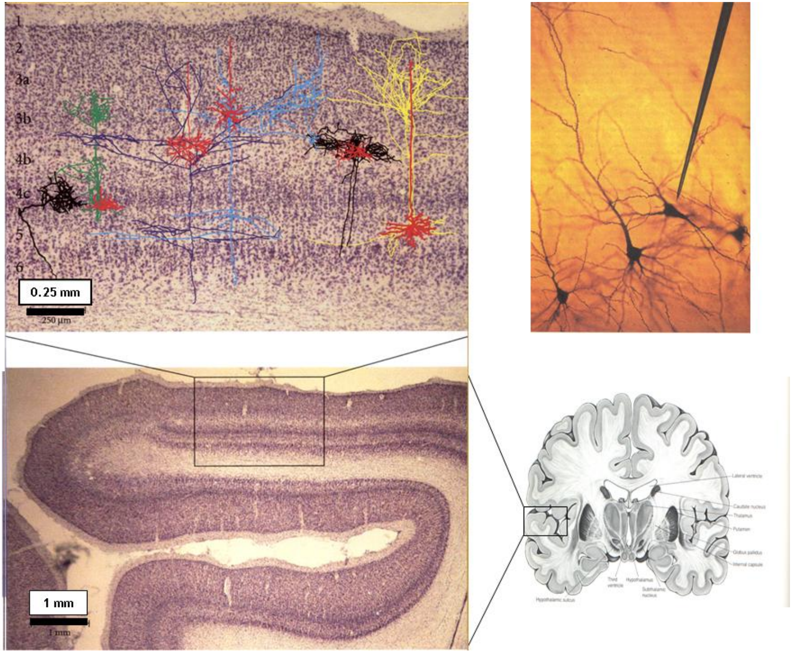

1
2
3a
3b
4b
4c
5
6
0.25 mm
250 µm
1 mm
1 mm
Lateral ventricle
Caudate nucleus
Thalamus
Putamen
Globus pallidus
Internal capsule
Third ventricle
Hypothalamus
Subthalamic nucleus
Hypothalamic sulcus

Brain building blocks

Mental activity due to network of nerve cells

- ~ 10^{11} nerve cells (neurons)
- ~ 10^{14} connections (synapses)
- cortex (humans):
  thickness ~ 2-4 mm
  area ~ 2000 cm^2

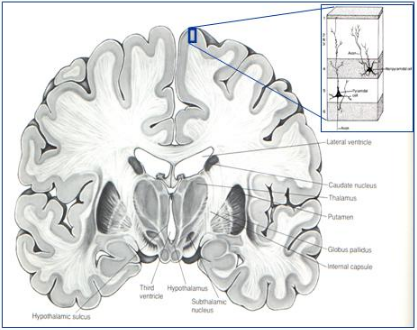

Smaller, but similar cortex in other mammals

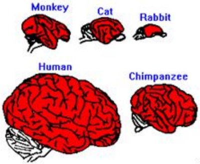

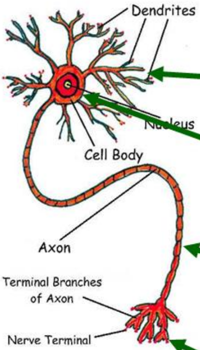

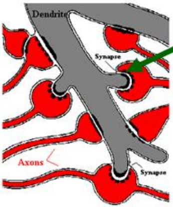

Signal processing in neurons

DENDRITE: Incoming signal spreads electrically to cell body (soma)

CELL BODY (SOMA): Fires an *action potential* if membrane voltage passes a threshold

AXON: Action potential propagates without damping to synapse (nerve terminal)

SYNAPSE: Diffusion of signal molecules (across synaptic cleft) modifies membrane voltage on receiving (postsynaptic) neuron

MATHEMATICAL DESCRIPTIONS AVAILABLE FOR ALL PROCESSES

Modelling at different levels of detail

Level		Problem		Tool
I	Detailed biophysical neuron	Neuron	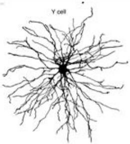	Computer simulation (ex. NEURON)
II	Simplified "spiking" neurons	Network	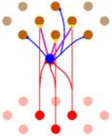	Computer simulation (ex. NEST)
III	Firing rate models	Network	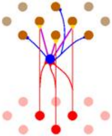	Analytical (+ numerical) mathematics

Rate equations and field theory

- Neuronal activity in population of neurons modeled in terms of firing rates P:

$$"Output = P(\sum Inputs)"$$

- Field theory $\leftrightarrow$ Separation of scales. Typical figure: $1mm^3$ brain tissue $\leftrightarrow 10^5$ neurons.
- Neurons in cortex group into two main categories:
  - Input from *excitatory (inhibitory)* neurons *increase (decrease)* the probability for the receiving neurons to fire action potentials
- Cortex contains approximately 80 % excitatory neurons, 20 % inhibitory neurons

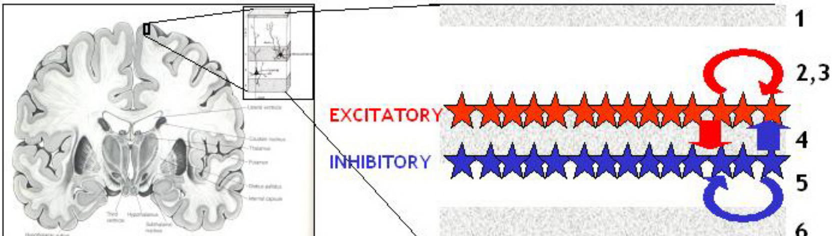

Two population model

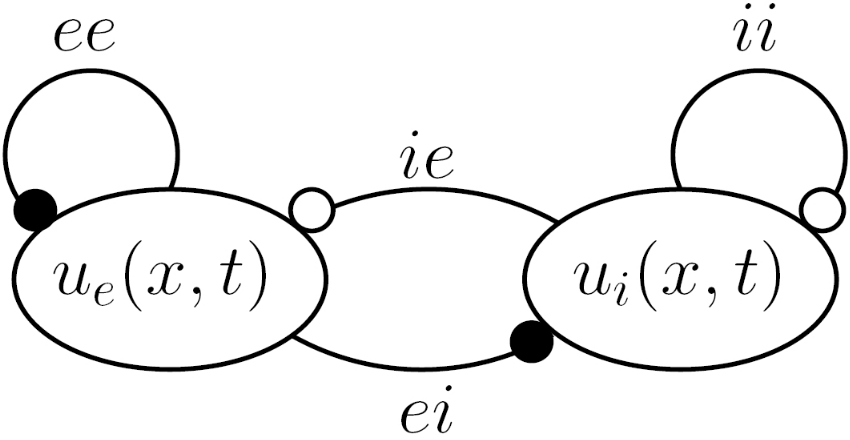

- Separate excitatory and inhibitory neurons into two distinct populations.
- One spatial dimension.
- No input sources.

Two population model

Two-population Volterra model [Coombes (2005), Wyller et al (2007a)]

$$
\begin{aligned}
u_e &= \alpha_{ee} * \omega_{ee} \otimes P_e(u_e - \theta_e) - \alpha_{ie} * \omega_{ie} \otimes P_i(u_i - \theta_i) \qquad (1)\\
u_i &= \alpha_{ei} * \omega_{ei} \otimes P_e(u_e - \theta_e) - \alpha_{ii} * \omega_{ii} \otimes P_i(u_i - \theta_i) \qquad (2)
\end{aligned}
$$

- ω_{mn} - norm., pos., bounded and symmetric connectivity functions

$$\omega_{mn}(x) = \frac{1}{\sigma_{mn}} \phi_{mn}\left(\frac{x}{\sigma_{mn}}\right)$$

- σ_{mn} - synaptic footprints

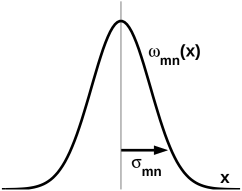

Two population model

Two-population Volterra model [Coombes (2005), Wyller et al (2007a)]

$$u_e = \alpha_{ee} * \omega_{ee} \otimes P_e(u_e - \theta_e) - \alpha_{ie} * \omega_{ie} \otimes P_i(u_i - \theta_i) \quad (1)$$

$$u_i = \alpha_{ei} * \omega_{ei} \otimes P_e(u_e - \theta_e) - \alpha_{ii} * \omega_{ii} \otimes P_i(u_i - \theta_i) \quad (2)$$

- P_m - firing rate functions

$$P_m(u_m) = \frac{1}{2}(1 + \tanh(\beta_m(u_m - \theta_m)))$$

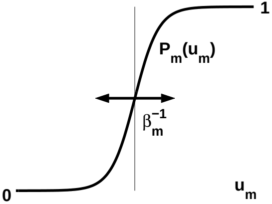

- β_m^{-1} - variation length of firing rate functions
- $0 < \theta_m \leq 1$ $(m = e, i)$ - threshold values for excitatory and inhibitory populations
  - α_{mn} - norm. temporal kernels modeling the time history of the network.
  - $[\omega_{mn} \otimes P_m(u_m - \theta_m)](x,t) = \int_{-\infty}^{\infty} \omega_{mn}(x - x')P_m(u_m(x',t) - \theta_m)dx'$.
  - $[\alpha_{mn} * \omega_{mn} \otimes P_m(u_m - \theta_m)](x,t) =$ $\int_{-\infty}^{t} \alpha_{mn}(t - s)[\omega_{mn} \otimes P_m(u_m - \theta_m)](x,s)ds$.

Bumps solutions in the Heaviside limit

[Blomquist et al (2005)]:

$$U_e(x) = W_{ee}(a-x) + W_{ee}(a+x) - W_{ie}(b-x) - W_{ie}(b+x)$$
$$U_i(x) = W_{ei}(a-x) + W_{ei}(a+x) - W_{ii}(b-x) - W_{ii}(b+x)$$
$$W_{mn}(x) \equiv \int_0^x \omega_{mn}(|z|)dz$$
$$U_e(\pm a) = \theta_e, \quad U_i(\pm b) = \theta_i \quad - \quad \text{pinning condition}$$

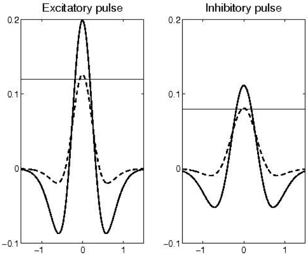

Time independent, spatial symmetric solutions in the Heaviside limit

[Blomquist et al (2005)]:

- **For all connectivity functions there is a subset of threshold values** (θ_e, θ_i) **for which bumps exist.**
- **Two pair of bumps** $(U_e(x), U_i(x))$ **for each set of threshold values** (θ_e, θ_i) **- "*broad pulse pair*"and "*narrow pulse pair*"**
- **Excitatory pulse may exist without accompanying inhibitory pulse. Inhibitory pulse cannot exist alone.**

Exponentially decaying kernels

- $\alpha_{ee}(t) = \alpha_{ie}(t) = e^{-t}$
- $\alpha_{ei}(t) = \alpha_{ii}(t) = \frac{1}{\tau} e^{-t/\tau}$, $\tau = \tau_i/\tau_e$.

$\tau_e(\tau_i)$ - typical timescale for excitatory (inhibitory) neurons.

$$\begin{aligned} \partial_t u_e &= -u_e + \omega_{ee} \otimes P_e(u_e - \theta_e) - \omega_{ei} \otimes P_i(u_i - \theta_i) \quad (3) \\ \tau \partial_t u_i &= -u_i + \omega_{ie} \otimes P_e(u_e - \theta_e) - \omega_{ii} \otimes P_i(u_i - \theta_i) \quad (4) \end{aligned}$$

A) Stability of bumps - Amari approach

[Blomquist et al (2005)]

- $P_n = H$: H - Heaviside function
- $u_e(a(t), t) = \theta_e$, $u_i(b(t), t) = \theta_i$
- $\partial_x u_e(a(t), t) \approx U_e'(a_{eq})$, $\partial_x u_i(b(t), t) \approx U_i'(b_{eq})$
- 2d autonomous dynamical system for (a, b).
- Equilibrium (a_{eq}, b_{eq}) of dynamical system $\leftrightarrow$ Bumps
- Stability of $(a_{eq}, b_{eq}) \rightarrow$ Stability of bumps

Results:

- **Narrow pulse pair: Unstable for all τ.**
- **Broad pulse pair: Stable for small and moderate values of τ, converted to breathers as τ exceeds a certain threshold $\leftrightarrow$ Supercritical Hopf bifurcation.**

B) Full stability analysis

- $P_n = H, \quad u_e(x,t) = U_e(x) + \chi(x,t), u_i(x,t) = U_i(x) + \psi(x,t) \quad +$ linearized evolution eqs. for $(\chi(x,t), \psi(x,t))$.
- $\chi(x,t) = e^{\lambda t}\chi_1(x)$, $\psi(x,t) = e^{\lambda t}\psi_1(x)$, λ growth/decay rate.
- $\mathbf{J}(\lambda) \cdot \underline{X} = \underline{0}, \quad \underline{X} = [\chi_1(a_{eq}), \chi_1(-a_{eq}), \psi_1(b_{eq}), \psi_1(-b_{eq})]^T$
- $\widetilde{\mathbf{J}}(\lambda) = \mathbf{P}\mathbf{J}(\lambda)\mathbf{P}^{-1}$

$$\widetilde{\mathbf{J}}(\lambda) = \begin{pmatrix} \mathbf{J}_A(\lambda) & \mathbf{0} \\ \mathbf{0} & \mathbf{J}_{NA}(\lambda) \end{pmatrix}$$

Evans function E:

$$E(\lambda) = det(\mathbf{J}(\lambda)) = 0 \Leftrightarrow det(\mathbf{J}_A(\lambda)) = 0, det(\mathbf{J}_{NA}(\lambda)) = 0$$

- $det(\mathbf{J}_A(\lambda)) = 0 \leftrightarrow$ Amari analysis, symmetric perturbations.
- $det(\mathbf{J}_{NA}(\lambda)) = 0 \leftrightarrow$ Non - Amari, $\lambda = 0$ (translation invariance of pulses), anti - symmetric perturbations.

Result: **Amari analysis gives correct predictions with one notable exception.**

- Excitatory pulse
- Inhibitory pulse

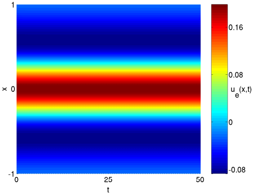

Stable Broad Pulse Pair
$(\tau < \tau_{cr})$

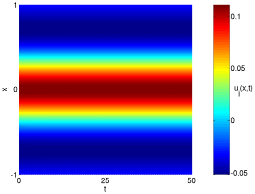

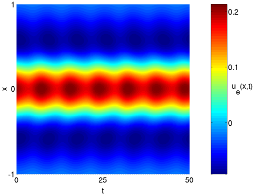

Oscillating Broad Pulse Pair
$(\tau \gtrsim \tau_{cr})$

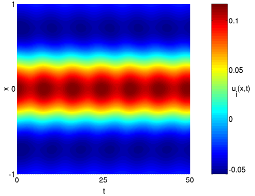

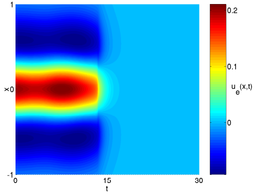

Collapsing Broad Pulse Pair
$(\tau \gg \tau_{cr})$

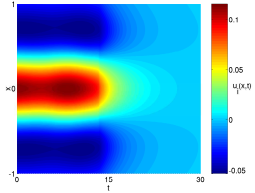

Turing type of instability - pattern formation

- Turing instability $\Rightarrow$ Generation of coherent structures like bumps and traveling waves.
- Existence of spatially homogeneous equilibrium u_{eq}.
- Additional spatial noise + nonlocal effects in (1) - (2) can generate patterns.

Pattern formation

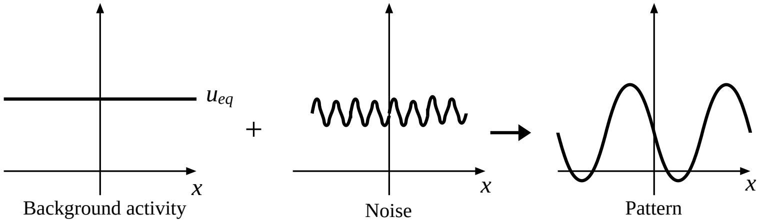

Linear analysis

[Wyller et al (2007b)]

- Existence of constant equilibrium $u_e(x,t) = u_i(x,t) = u_{eq}$.
- Linear stability analysis of equilibrium of local limit $\omega_{mn} \to \delta$.
- Linear stability analysis of equilibrium in the general case
- $u_e(x,t) = u_{eq} + \phi(x,t)$, $u_i(x,t) = u_{eq} + \psi(x,t)$.
- Linearized nonlocal evolution equations for (ϕ, ψ).
- $(\hat{\phi}, \hat{\psi})$- Fourier transforms of (ϕ, ψ), k, wave number of Fourier - comp. of (ϕ, ψ):

$$\partial_t \underline{X} = \mathbf{A}(\eta) \cdot \underline{X}, \quad \underline{X} = [\hat{\phi}, \hat{\psi}]^T, \quad \eta = k^2$$

- Stability problem $\leftrightarrow \underline{\gamma}(\eta) = (tr(\mathbf{A}(\eta)), det(\mathbf{A}(\eta)))$
  - $k = 0 \Leftrightarrow$ Local limit $\omega_{mn} \to \delta$
  - $|k| \to \infty \Rightarrow tr(\mathbf{A}(\eta) < 0, det(\mathbf{A}(\eta)) > 0$

Result: **Finite bandwidth instability consisting of a countable set of well separated gain bands for smooth spectra of connectivity functions.**

Example: Shallow slope firing rate functions - linear stage

$$\omega_{mn}(x) = \frac{1}{2\sigma_{mn}} \exp(-|x|/\sigma_{mn}), \quad m,n = e,i$$

Trace - Determinant

Growth rate

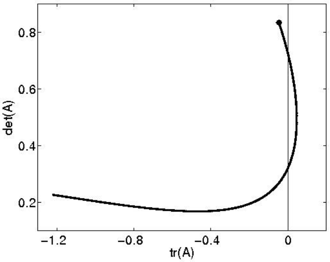

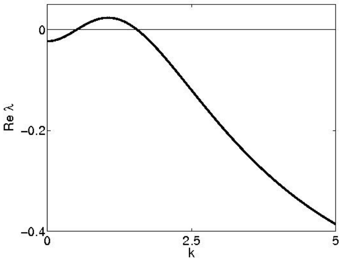

Example: Shallow slope firing rate functions - numerical simulations

Excitatory level

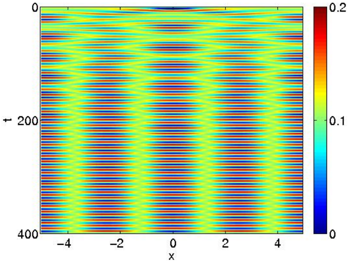

Inhibitory level

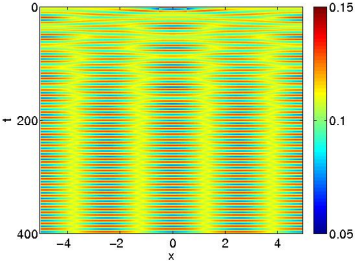

Example: Steep firing rate functions - linear stage

$$\omega_{mn}(x) = \frac{1}{2\sigma_{mn}} \exp(-|x|/\sigma_{mn}), \quad m, n = e, i$$

Trace - Determinant

Growth rate

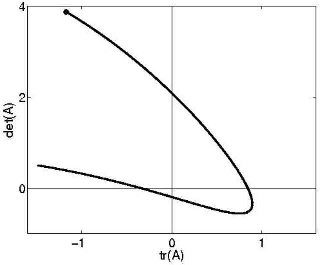

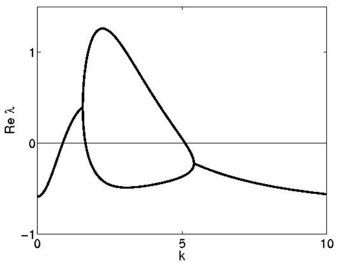

Example: Steep firing rate functions - numerical simulations

Excitatory level | Inhibitory level

a)

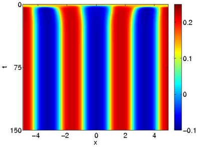

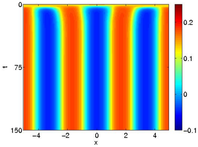

Excitatory bump | Inhibitory bump

b)

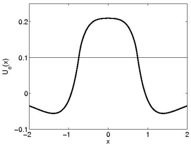

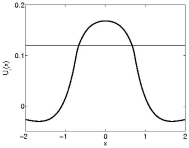

- **Experimental findings:** Primary visual cortex (V1) is not homogeneous and isotropic. It has a periodic microstructure on the millimeter length scale.
- **Modelling framework:**

$$\omega_{mn}(|x|) \to \omega_{mn}^{(\varepsilon)}(x) \equiv \omega_{mn}(x, \tfrac{x}{\varepsilon}), \quad 0 < \varepsilon \ll 1$$

$$\omega_{mn} - 1 \text{ - periodic in second variable}$$

$$\frac{\partial}{\partial t} u_e^{(\varepsilon)} = -u_e^{(\varepsilon)} + \omega_{ee}^{(\varepsilon)} \otimes P_e(u_e^{(\varepsilon)} - \theta_e) - \omega_{ie}^{(\varepsilon)} \otimes P_i(u_i^{(\varepsilon)} - \theta_i)$$

$$\tau \frac{\partial}{\partial t} u_i^{(\varepsilon)} = -u_i^{(\varepsilon)} + \omega_{ei}^{(\varepsilon)} \otimes P_e(u_e^{(\varepsilon)} - \theta_e) - \omega_{ii}^{(\varepsilon)} \otimes P_i(u_i^{(\varepsilon)} - \theta_i)$$

- **Problem:** Asymptotic limit $\varepsilon \to 0$.
  Solution: Multiscale convergence technique (Nguetseng, 1989) + Two - scale convergence of convolution integrals (Visintin, 2007)

$$\frac{\partial}{\partial t} u_e = -u_e + \omega_{ee} \otimes \otimes P_e(u_e - \theta_e) - \omega_{ie} \otimes \otimes P_i(u_i - \theta_i)$$

$$\tau \frac{\partial}{\partial t} u_i = -u_i + \omega_{ei} \otimes \otimes P_e(u_e - \theta_e) - \omega_{ii} \otimes \otimes P_i(u_i - \theta_i)$$

$$[f \otimes \otimes g](x, y) \equiv \int_{\Omega} \int_{Y} f(x - x', y - y') g(x', y') dy' dx'$$

Y - period cell

Problem: Existence and stability of bumps when

$$\omega_{mn}(x, y) = \sigma_{mn}^{-1}(y) \Phi[\frac{x}{\sigma_{mn}(y)}]$$

$$\sigma_{mn}(y) = s_{mn}(1 + \alpha_{mn} \cos(2\pi y)), \quad s_{mn} > 0, \quad 0 \le \alpha_{mn} < 1$$

$$P_m = H \quad - \quad \text{Heaviside function}$$

$$\alpha_{mn} \quad - \quad \text{degree of heterogeneity}$$

- **Existence of bumps:** Pinning function technique as in the translational invariant case.
- **Stability methodology:** Fredholm integral operator, block diagonalization of this operator, Fourier - decomposition technique produces sequences of Evans - functions.
- **Results:**
  1. Same result as in the translational invariant case for the weakly modulated case ($0 < \alpha_{mn} \ll 1$).
  2. Beyond the weakly modulated case: Rich plethora of phenomena, numerical detection of three bumps pairs where at least one bumps pair (and maximum two bumps pairs) are stable for small values of the relative inhibition time.

Conclusions

- Two pair of bumps for each set of threshold values
  - Broad pulse pair stable for small and moderate values of relative inhibition time, unstable above a certain threshold
  - Narrow pulse pair unstable
- Pattern formation through a Turing type of instability.
- Spatial oscillations for steep firing rate functions, each period identified with a bump.
- Spatio - temporal oscillations for shallow firing rate functions.
- Existence and stability of bumps in a two - population homogenized Amari model: A rich plethora of phenomena.

Some references

- Blomquist et al (2005), *Localized activity patterns in two-population neuronal network*, Physica D **206**, 180, (2005).
- Wyller et al (2007a): Biophysical Reviews and Letter, *On the Origin and Properties of Two-Population neural Field Models - A Tutorial Introduction*, **2**, No. 1, January 2007.
- Wyller et al (2007b) *Turing instability and pattern formation in a two-population neuronal network model*, **225**, 75,(2007).
- Nguetseng, *A general convergence result of a functional related to the theory of homogenization*, SIAM J. Math. Anal. 20 (1989) 608–623.
- Visintin, *Towards a two-scale calculus*, ESAIM: COCV, 12 (2006) 371–397.
- Svanstedt et al, *Homogenization of a Wilson - Cowan model for neural fields in a bounded domain*. Nonlinear Analysis: Real World Applications 14 (2013) 1705–1715.

Some references, cont.

- Svanstedt et al, *A one population Amari - model with periodic microstructure*, Nonlinearity 27(2014) 1391–1417.
- Malyutina et al, *Two bump solutions of a homogenized Wilson - Cowan model with periodic microstructure*, Physica D 271 (2014) 19–31.
- Coombes et al, *Waves in random neural media*, Discrete and Continuous Dynamical Systems — Series A, 32 (2012) 2951–2970.
- Malyutina et al, *Numerical analysis of bump solutions for neural field equations with periodic microstructure*, Applied Mathematics and Computation 260 (2015) 370 – 384.
- Burlakov et al,*Two-dimensional Amari neural field model with periodic microstructure: Rotationally symmetric bump solutions*, Communications in Nonlinear Science and Numerical Simulation 32 (2016) 81 – 88.
- Kolodina et al,*Single bumps in a 2 - population homogenized neuronal network model*, Under preparation. May 2017.
- Coombes, Biological Cybernetics, *Waves, bumps, and patterns in neural field theories*, Biological Cybernetics **93**, 91, (2005).